Modelling Fluid Dynamics, Heat Transfer and Valve Dynamics in a Reciprocating Compressor

by:

Roland Aigner and Herbert Steinrück
Institute of Fluid Dynamics and Heat Transfer
Vienna University of Technology
Vienna
Austria
roland.aigner@tuwien.ac.at

5th Conference of the EFRC
March 21-23, 2007
Prague, Czech Republic

Abstract:

In the present study one- and two-dimensional numerical models are proposed for calculating gas flow and valve dynamics in a reciprocating compressor. It turns out that they are capable of capturing the most important physical effects during a compression cycle, namely the interaction between pressure waves inside the cylinder and valve dynamics. In order to model the heat transfer from the gas to the cylinder full three-dimensional simulations have been carried out. Inspecting the results a reconstruction of the heat flux depending only on few dimensionless numbers has been derived. The reconstructed heat fluxes have been incorporated into the simplified one dimensional compressor model allowing a heat transfer analysis of a compression cycle. Comparisons with measurements and full three-dimensional simulations of different types of compressors show good agreement.

1 Introduction

Full three-dimensional simulations of reciprocating compressors with present commercial CFD-programs are state of the art. They produce accurate and reliable results regarding valve motion, fluid dynamics and heat transfer. But, they cannot meet the demands of engineers for usability and short computation times. For example the average computation time for one compression cycle inside the cylinder can exceed 2 days[1].

At first glance calculating the gas flow in a compressor seems to be a complicated task and a full three-dimensional simulation unavoidable. However, it turns out that a quasi one-dimensional model for the gas flow coupled to a simple valve model is sufficient to describe the main effects in case of barrel design compressors with two valves. Compressors with more than two valves require a quasi two-dimensional approach in order to account for the multiple valve pockets, where the gas enters and leaves the cylinder. Apart from the fact that both the quasi one-dimensional model and the quasi two-dimensional model need remarkable less computation time than the full simulation, only the main features of the compressor geometry have to be specified.

Considering heat transfer one can perform on one hand a full three-dimensional numerical simulation including the heat transfer analysis of the mechanical structure, the exchange of heat with the environment and heat transfer processes in the compressor as well. The disadvantages of such an approach are stated above. On the other hand one can use some empirical estimates of the heat transfer from the gas to the compressor. These formulas are naturally very crude since they cannot be expected to capture the heat transfer process within the cylinder which depends on complex flow processes. Therefore the following approach combining both methods will be used. By means of well proven commercial CFD codes the heat transfer is determined for a wide range of compressor types and operating parameters. Inspecting the results and furthermore identifying the major physical effects of the heat transfer leads to reconstructed heat fluxes, whereas the reconstruction is based on a few dimensionless numbers and some process quantities such as gas temperature inside the cylinder and mass flow.

First we introduce the quasi one-dimensional and two-dimensional flow model. Since the quasi one-dimensional model was presented in detail in 2005 at the 4th EFRC conference[2] this paper focuses on the two-dimensional approach and compares simulation results with measurements. Then the heat transfer reconstruction method will be derived. And finally we present an extension of the well-proven one-dimensional simulation tool for two-dimensional geometries and heat transfer analysis.

2 Modelling of the Gas Flow and Valve Dynamics

2.1 Geometry

2.1.1 Three-dimensional

Half of the interior of a reciprocating compressor is displayed schematically in figure 1. The piston is shown at an intermediate position, where it does not mask the valve pockets. The valves are adjacent to the circular lateral surfaces of the valve pockets.

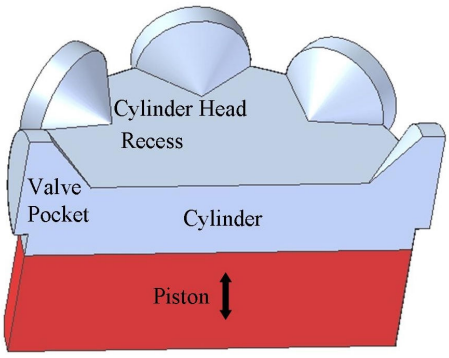

Figure 1: Geometry of compressor with more than two valves

2.1.2 One-dimensional

In the quasi 1-d model the wave propagation along the diameter (x-axis) of the cylinder from the suction to the pressure valve is considered. The equations of motion (Euler equations) are integrated over a cross section $A(x,t)$ perpendicular to the x-axis. The effective cross sections of the quasi one-dimensional model are displayed schematically in figure 2.

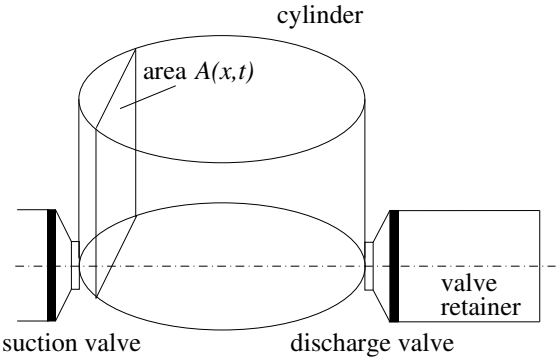

Figure 2: Schema of the one- dimensional model

2.1.3 Two-dimensional

The two-dimensional model takes the wave propagation in a plane parallel to the cylinder head (x,y-plane) into account. The equations of motion (Euler equations) are integrated over the height *h(x,y,t)* of the cylinder. In terms of the compressor the height is the distance between the piston and the cylinder head. The two-dimensional computational domain is displayed schematically in figure 3.

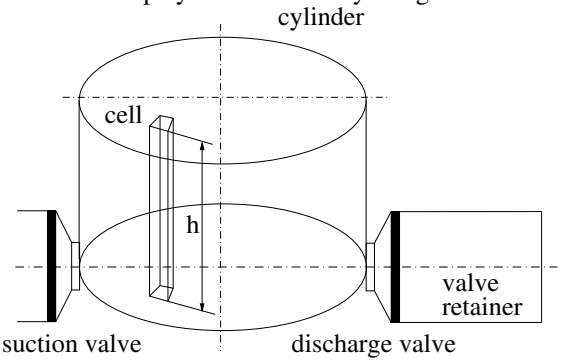

Figure 3: Schema of two-dimensional model

In order to keep the model as simple as possible and hence least time consuming (in terms of computational time) a one-dimensional approach is used for the valve pockets and valve retainers. A typical grid for a compressor with eight valves is shown in figure 4.

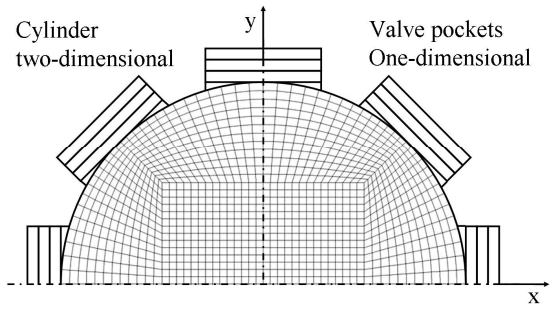

Figure 4: Combined two-dimensional one-dimensional grid

2.2 Governing Equations

2.2.1 Piston Motion

The distance between piston and cylinder head h depending on time t can be determined using the properties of the crank mechanism. We use the length of the crank lever r, the length of the piston rod l, the smallest distance between piston and cylinder top h_0 an the present angle of the crankshaft φ to obtain

$$h = r + l + h_0 - r\cos\varphi - l\sqrt{1-\left(\frac{r}{l}\right)^2 \sin^2\varphi}\,, \qquad (1)$$

where $\varphi=2\pi nt$. Here, n denotes the speed of the crankshaft.

2.2.2 Flow Field

The governing equations for the flow of gas are obtained by taking the mass and momentum balance over a cell. The variables ρ, u, v, p have their usual meaning, density, velocity in x-direction, velocity in y-direction and pressure, respectively.

$$\frac{\partial \rho h}{\partial t} + \frac{\partial \rho u h}{\partial x} + \frac{\partial \rho v h}{\partial y} = 0\,, \qquad (2)$$

$$\frac{\partial \rho u h}{\partial t} + \frac{\partial (\rho u^2 h + p h)}{\partial x} + \frac{\partial (\rho v u)}{\partial y} = p\frac{\partial h}{\partial x}\,, \qquad (3)$$

$$\frac{\partial \rho v h}{\partial t} + \frac{\partial (\rho v^2 h + p h)}{\partial y} + \frac{\partial (\rho v u)}{\partial x} = p\frac{\partial h}{\partial y}\,. \qquad (4)$$

Assuming isentropic flow conditions we replace the energy equation with

$$p\rho^{-\gamma} = \text{const}\,, \qquad (5)$$

where γ denotes the ratio of specific heat capacities. Note that equations (3) and (4) are not of conservation form. The right hand terms constitute a momentum source of the flow due to a variation of the height inside the cylinder. However, only smooth cylinder head recesses can be considered since the gradients of h become very large in case of sharp changes.

The governing equations (2)-(4) reduce to the one-dimensional model equations by replacing the height h with the cross-section A and setting the velocity in y-direction v to zero.

2.2.3 Valve Dynamics

The treatment of valve motion follows the well known Costagliola[3] theory. The state of a valve is specified by the distance between valve plate and seating (valve lift) x_v. The motion of the valve plate is determined by the forces acting on it. We consider the following three contributions to the resulting force: the pressure difference across the valve acting on an effective force area A_v of the valve plate, the springing and thirdly a contribution due to viscous forces in the initial stages of valve opening. Denoting the pressure in front of the valve p_1 and behind the valve p_2 we obtain the equation of motion for the valve plate

$$m_v \ddot{x}_v = (p_1 - p_2)A_v - k(x_v + l_1) - F_{adh}. \qquad (6)$$

Here m_v stands for the mass of the valve plate. The constants k and l_1 denote stiffness of springing and initial deflection of the springs. An initial sticking effect is modelled by the force F_{adh}. It is caused by the viscosity of the gas in the valve gap resulting in a small time delay when the valve is opening. It reads as follows (Flade[4])

$$F_{adh} = f_1 \frac{\dot{x}_v}{x_v^3}. \qquad (7)$$

The factor f_1 depends on geometric features of the valve and properties of the gas. It also takes lubrication oil at the valve plate into account.

2.2.4 Flow through the valve

The flow through the valve is considered as the (quasi stationary) outflow of a gas from a pressurized vessel through a convergent nozzle. The mass flow through the valves is given by St.Venant and Wantzell[4],

$$\dot{m} = \phi \rho_1^0 \left(\frac{p_2}{p_1^0}\right)^{\frac{1}{\kappa}} \sqrt{\frac{2\kappa}{\kappa-1}\frac{p_1^0}{\rho_1^0}\left(1-\left(\frac{p_2}{p_1^0}\right)^{\frac{\kappa-1}{\kappa}}\right)}. \qquad (8)$$

where p_1^0 is the totel pressure before and p_2 is the pressures after the valve, respectively.

The effective flow cross section ϕ of the valve is assumed to be a function of the position of the valve plate x_v only. It has to be determined empirically.

2.3 Numerical Solution

2.3.1 Finite Volume Method

For the numerical analysis it is useful to write the continuity equation (2) and both equations of motion (3), (4) in following form:

$$\frac{\partial \mathbf{u}}{\partial t} + \frac{\partial \mathbf{f}(\mathbf{u}, x)}{\partial x} = \mathbf{s}, \qquad (9)$$

with the state vector $\mathbf{u} = (\rho A, u\rho A, v\rho A)^T$. $f(\mathbf{u},x)$ and $\mathbf{s}$ denote flux functions and source functions, respectively. In case of the one-dimensional approach the state vector $\mathbf{u}$ is reduced to $(\rho A, u\rho A)^T$ and appropriate flux functions and source functions are used.

The system of equations (9) can be solved by different finite volume schemes. The f-wave algorithm by Leveque[5] and the Lax-Wendroff[6] scheme can be applied to the one-dimensional approach and the two-dimensional method, respectively.

2.3.2 Boundary and Interface Conditions

The finite volume scheme has to be supplied with appropriate boundary conditions. If the valves are closed, they are described as a fixed wall, by setting u=0. If the valve is open the mass flow is prescribed. It is obtained by equation (8) as a function of the total pressures before and after the valve and the valve plate position. The pressure outside the suction valves is kept constant. To determine the pressure after the discharge valves wave propagation in the valve retainers are computed using the finite volume scheme. At the end of the valve retainer the pressure is prescribed. The equation of motion (6) of the valve plate is solved simultaneously by an explicit second order scheme.

Every opening or closing valve initiates a wave. Thus, in case of compressors with more than two valves two-dimensional wave patterns occur, which cannot be approximated by plane waves. Extending the model for the numerical simulation inside the cylinder to two dimensions resolves this problem. However interface conditions must be set for the transition from the one-dimensional domain to the two-dimensional domain.

Regarding our model the interfaces are located between the valve pockets and the cylinder.

2.3.3 Time step

The time step Δt of the numerical integration has to be chosen such that the stability conditions of the numerical schemes are satisfied. In case of the one-dimensional approach the CFL condition $\Delta t<\Delta x/(c+|u|)$ has to hold, where Δx is the interval length of the spatial discretization and c is the velocity of sound. In the two-dimensional case we limit the time step by $\Delta t<\Delta x/(c+|u|+|v|)$. Using an explicit scheme for the valve dynamics the numerical stability condition $\Delta t < m_v/k$ must be satisfied.

2.4 Comparison of the Numerical Solution with measured Data

2.4.1 Compressor with 2 valves

A double acting, 2 cylinders, barrel design reciprocating compressor was tested at Burckhardt Compression, Switzerland. The main specifications of the compressor can be found in table 1. Pressure sensors inside the cylinder (see figure 5) record the pressure at different locations. The relative pressures in the diagrams are referred to an ambient pressure of 0.97 bar.

Type of compressor	Burckhardt Compression 2K90-1A: 2 cylinders, double acting
Bore diameter	0.22 m
Stroke	0.09 m
Speed of Crankshaft	980 ÷ 990 rpm
Gas	Air
Number of Valves	2
Pressure Ratio	1/2 and 1/5

Table 1: Main specifications of theBurckhardt test compressor

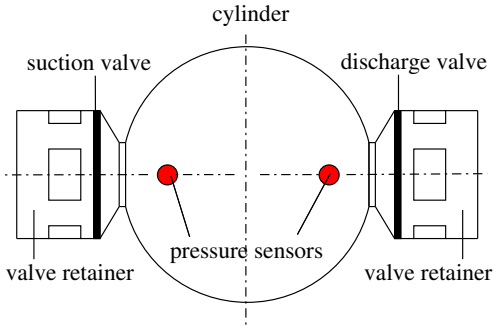

Figure 5: Position of pressure sensors

In figure 6 comparisons of the measured pressures at two positions with the numerical solution of the quasi one-dimensional model for discharge pressures of 5 bar and 2 bar are given. Figure 7 shows the appropriate comparison of the valve motion. Since the pressure distribution and valve motion are in a very good agreement with measurements we expect that the bulk temperature inside the cylinder and mass flow are also well represented. For more details of the flow behaviour we refer to [2].

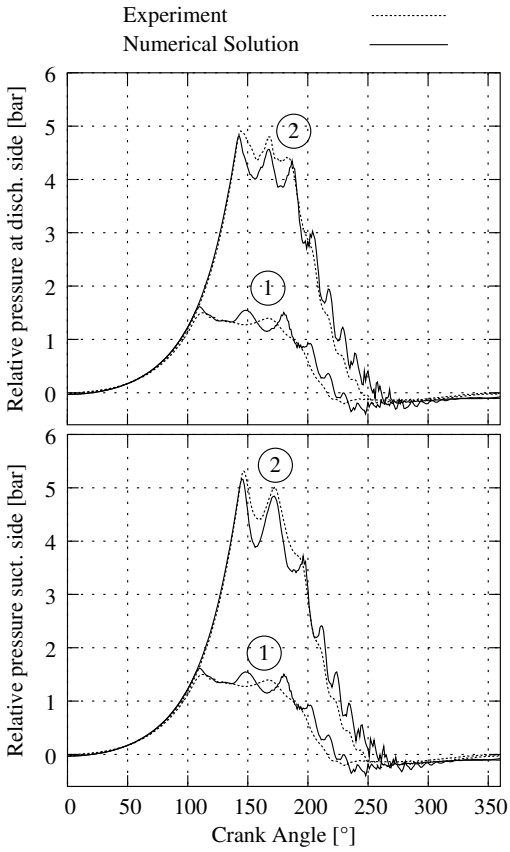

Figure 6: Comparison of the numerical solution of quasi one-dimensional model and measurements, a) pressure at discharge valve, b) pressure at suction valve for discharge pressures of 2 bar (curves 1) and 5 bar (curves 2)

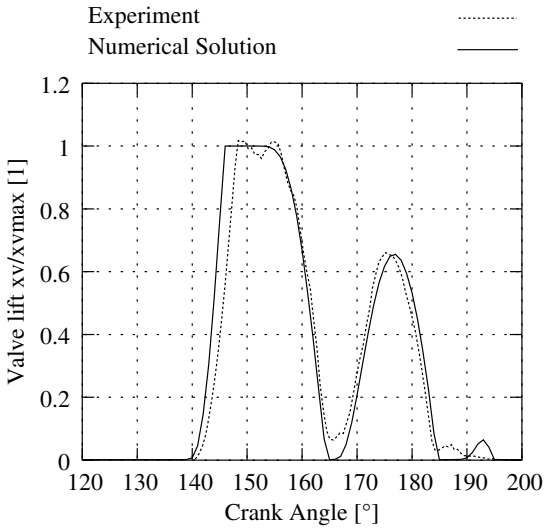

Figure 7: Comparison of the numerical solution of the quasi one-dimensional model and measurements; valve lift for discharge pressures of 5 bar

2.4.2 Compressor with 8 valves

The main specifications of the Ariel JGD 26.5 – test compressor can be found in table 2. The location of pressure sensors are marked in figure 8.

Type of compressor	Ariel JGD 26.5
Bore diameter	0.673 m
Stroke	0.14 m
Speed of Crankshaft	1182 rpm
Gas	Nitrogen
Number of Valves	8
Pressure Ratio	2.2/6.4

Table 2: Main specifications of the Ariel test compressor

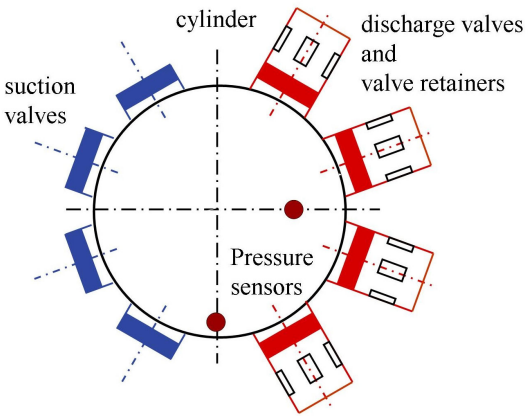

Figure 8: Position of pressure sensors

Figure 9 shows the pressure at the two locations inside the cylinder during a working cycle. Comparing measurements with numerical data shows a very good agreement.

The pressure distribution inside the cylinder shortly after the discharge valves has opened is displayed in figure 10. Since the wave fronts strongly deviate from plane waves a two-dimensional approach is necessary.

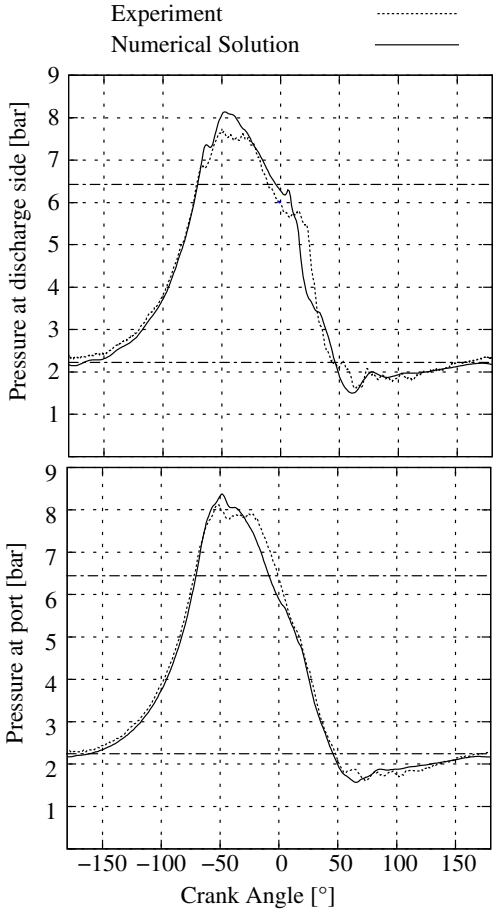

Figure 9: Comparison of the numerical solution of the quasi 2-d model and experiment, a) pressure at discharge side, b) pressure between discharge and suction side. Dash-dotted lines represent suction and discharge pressure, respectively

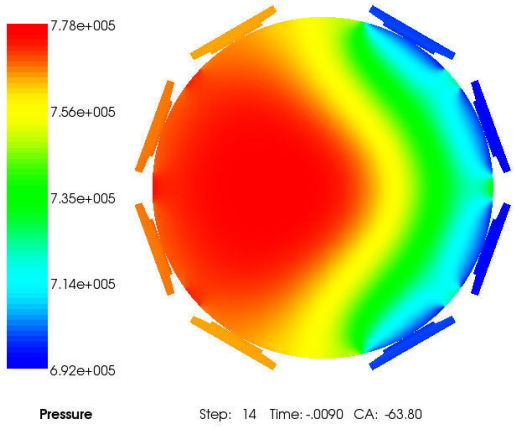

Figure 10: Pressure distribution inside cylinder shortly after opening of discharge valves (Screenshot of Compressor2d)

3 Modelling of the Heat Transfer

The essential part of the heat supply to the compressor is due to the temperature rise of the compressed gas during compression. Thus the main contribution to the heat balance of a reciprocating compressor is the heat transfer from the gas to the mechanical structure, e.g. the cylinder shell, the piston, the cylinder head and piston rod to name the most prominent surfaces of the compression chamber. It is essential to find the heat fluxes for the individual surfaces of the compression chamber.

3.1 Method

First the heat fluxes and heat transfer coefficients from the gas to the compressor have been determined for a sufficient number of cases by means of full three-dimensional numerical simulations. Next the heat fluxes through the individual faces are reconstructed by an ansatz which depends only on few dimensionless parameters. Finally correlations between these dimensionless parameters and the process parameters have been established.

3.2 Reconstruction

The basic idea of the reconstruction is to relate the local heat flux density $\dot{q}$ to a sum of weighted reference enthalpy flux densities $\dot{h}_{ref,i}$. It is defined by

$$\dot{q} = \sum_i \mathrm{St}_i \dot{h}_{ref,i} = \sum_i \mathrm{St}_i c_p \rho_{ref,i} u_{ref,i} \Delta T \,, \qquad (10)$$

where St_i can be interpreted as Stanton numbers and ΔT is a characteristic temperature difference. c_p stands for specific heat capacity at constant pressure. The reference value for the flow velocity $u_{ref,i}$ and the reference value for the density $\rho_{ref,i}$ depend on the physical effect i which contributes to the heat flux density. An educated understanding of the flow behaviour is essential in order to set suitable reference values. In terms of heat transfer three different phases during one working cycle can be distinguished; Inflow, Outflow and Compression/ Expansion.

3.2.1 Inflow

The gas enters through the suction valve. We expect a jet of cold gas emanating at the suction valve and impinging onto the piston rod or surfaces adjacent to the suction valve. We extract the reference velocity from the inlet mass flow $\dot{m}_{in}$ through the suction valve:

$$u_{ref,in} = \dot{m}_{in} / \rho_{in} A_{cross} \,, \qquad (11)$$

where A_{cross} is the cross section of the compression chamber along the piston rod. The density ρ_{in} is the density of the thermodynamic state of the gas at inflow. The heat transfer will be affected only after some retardation time t_0 since it takes some time that the cold gas impinges at the surfaces of the compression chamber. Thus the associated heat flux through a surface of area $A(t)$ of the compression chamber as a function of the time t takes the form

$$\dot{Q}_{in}(t) = \mathrm{St}_{in}\, c_p (T_w - T_{gas}) \frac{A(t)}{A_{cross}(t)} \dot{m}_{in}(t - t_0) \,. \qquad (12)$$

3.2.2 Outflow

During outflow we expect that the flow is dominated by the outflow of the gas. Similar to the inflow phase we approximate the heat flux by

$$\dot{Q}_{out}(t) = \mathrm{St}_{out}\, c_p (T_w - T_{gas}) \frac{A(t)}{A_{cross}(t)} \dot{m}_{out}(t) \,. \qquad (13)$$

For the outflow no retardation is necessary since the information that the valve is open spreads with the velocity of sound which is considerable large compared to the actual flow velocity.

3.2.2 Compression / Expansion

In the compression phase a natural reference velocity is the actual velocity of the piston $u_p(t)$. However, at the turning points of the piston motion it is zero but the heat flux density will not vanish. Thus we use the mean piston velocity u_m as reference velocity during that phase. As reference density we use the density $\rho_{isen}(T)$ which results from an isentropic change of state from the inflow condition (ρ_{in}, T_{in}) to the actual gas temperature T_{gas} in the compressor. The corresponding component of the heat flux can be written as

$$\dot{Q}_{ce}(t) = \left(\mathrm{St}_p\, u_p(t) + \mathrm{St}_m\, u_m\right)\rho_{isen}(T_{gas})\, c_p\,(T_w - T_{gas})\,A(t) \tag{14}$$

3.3 Reconstructed Heat Flux and Heat Flux Coefficient

Adding all components the total reconstructed heat flux is given by

$$\dot{Q}_{rec} = \dot{Q}_{in} + \dot{Q}_{out} + \dot{Q}_{ce}\,,$$

and the corresponding reconstructed heat transfer coefficient can be obtained from

$$\alpha = \frac{\dot{Q}_{rec}}{(T_W - T_{gas})A(t)}\,. \tag{15}$$

In this study the main surfaces of the compression chamber are considered, namely the piston, the cylinder head, piston rod and the cylinder shell. All other surfaces can be added to one of these.

3.4 Matching the nondimensional numbers $\mathrm{St_{in}}$, $\mathrm{St_{out}}$, $\mathrm{St_p}$, $\mathrm{St_m}$

The unknown dimensionless numbers $\mathrm{St_{in}}$, $\mathrm{St_{out}}$, $\mathrm{St_p}$, $\mathrm{St_m}$ are chosen such that for a given set of process parameters the reconstructed heat flux approximates the numerically computed heat flux best. Thus we minimize a functional which measures the distance between $\dot{Q}_{num}$ and $\dot{Q}_{rec}$.

3.5 Example

In this section the results of a heat transfer calculation are discussed. The input data and specifications for the calculation are taken from the two valve test case (table 1) using a simplified valve model; when the valve has opened completely it is kept open until the piston reaches the dead centre (see section 2.4.1).

The full three-dimensional calculation has been performed and the reconstructed heat fluxes have been derived. Figure 11 shows all components of the heat flux through the cylinder head. $\dot{Q}_{in}$, $\dot{Q}_{out}$, $\dot{Q}_p$ and $\dot{Q}_m$ contribute 3%, 16%, 18% and 63% to the total heat flux. In figure 12a the reconstructed heat flux through the cylinder head is compared to the numerical one. In figure 12b this comparison is shown for the heat transfer coefficient as well. As usual we choose the sign of the heat flux to be negative, if the heat flux vector is pointing out of the compression chamber.

Figures 11 and 12 show that at the beginning of the compression phase the heat flows from the surrounding material to the gas. From 640 °CA on the wall temperature is lower than the gas temperature and heat flows from the gas to the wall. During discharge phase (675 – 720°CA) the heat coefficient is increased due to higher velocities in the cylinder and therefore the negative heat flux is rising simultaneously. When the valve is closed, the velocity in the cylinder becomes very low and the heat transfer coefficient drops to the lower level again. Not until the suction valve opens the heat transfer coefficient will not increase. Due to expansion the gas is cooler than the wall from 750°CA on and the wall heats up the gas again. During suction phase the velocity inside the cylinder is smaller than the velocity during discharge phase. However a slight increase in heat flux coefficient and thus a rise in the heat flux are recognized.

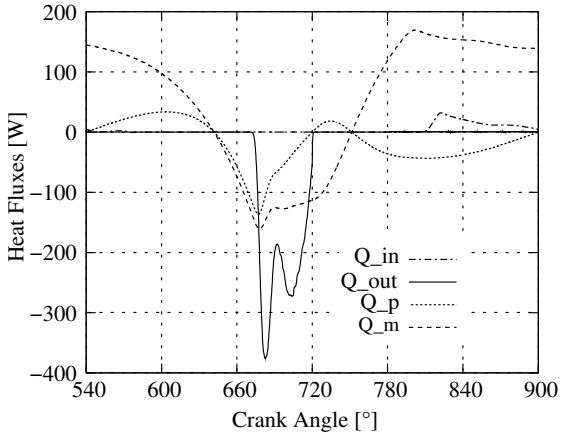

Figure 11: Heat flux through the cylinder head. Contributing components of reconstructed heat flux

In figure 13 the reconstructed heat flux through the side wall of the compressor is compared to the full three-dimensional data. Similar to figure 12 the heat fluxes or heat transfer coefficients are very well represented by the reconstructed ones. The area of the cylinder shell changes with time. When the piston approaches the dead centre high heat flux densities (due to high temperatures and heat transfer coefficients) meet only a small area and therefore the overall heat flux through the cylinder shell is only a fraction of the heat exchange at the cylinder head.

In general all statements for the cylinder head and the cylinder shell can be applied to the piston and the piston rod, respectively.

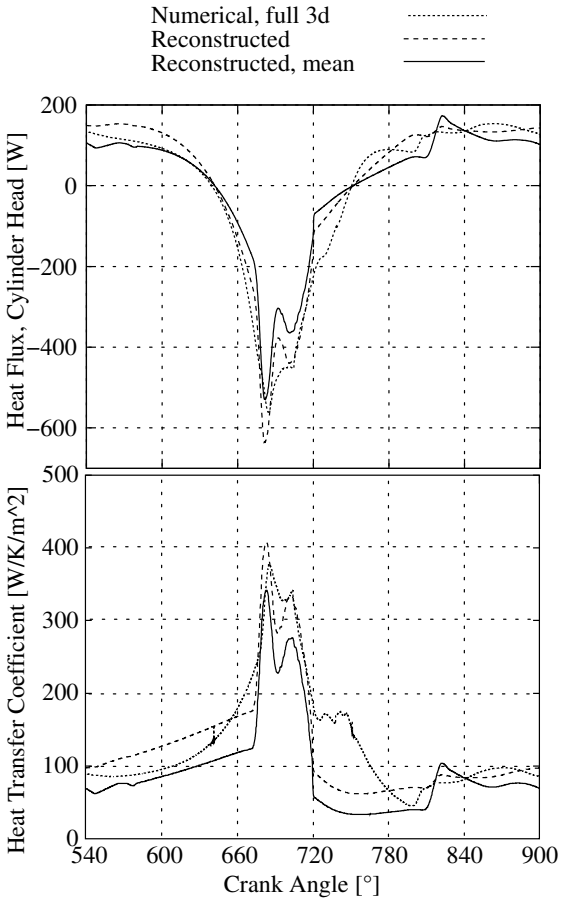

Figure 12: Heat flux through cylinder head (a) and associated heat transfer coefficient (b)

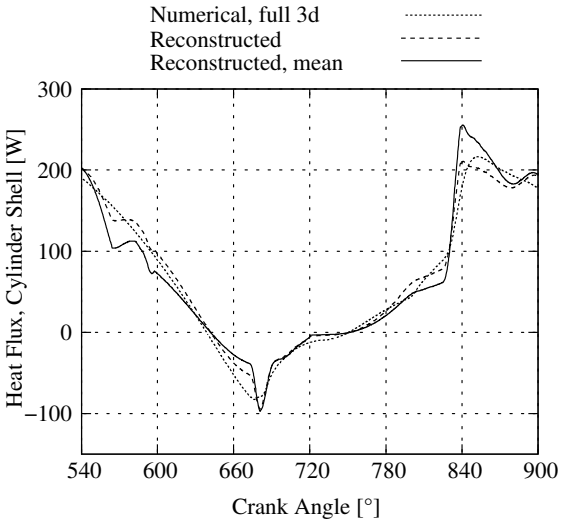

Figure 13: Heat flux through side wall of cylinder

3.6 Correlation between Reconstructed Heat Flux and Process Parameters

Reconstruction of the heat flux and determination of the Stanton numbers were conducted in more than 24 cases. Figure 13 displays St_m for the cylinder head over the Reynolds number $Re=u_m\rho_{in}D/\mu$.. It turns out that suitable average values of the Stanton numbers give very good results for the heat fluxes (figure 12 and 13; reconstructed mean). Thus universal Stanton numbers were found minimizing the functional which measures the distance between $\dot{Q}_{num}$ and $\dot{Q}_{rec}$ for all the simulated cases simultaneously.

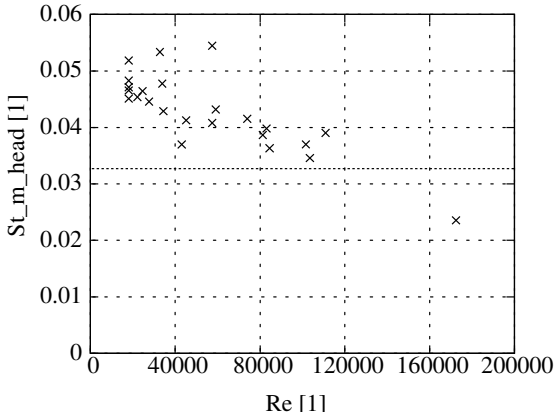

Figure 14: Stanton number St_m for the cylinder head for 24 different cases. Mean value of St_m is represented by dotted line

4 Simulation Tool

The one-dimensional and two-dimensional flow models which describe the pressure waves inside the cylinder and their interaction with the valve dynamics are incorporated in two user-friendly programs called Compressor1d and Compressor2d.

In order to determine the heat transfer coefficients besides the thermodynamic properties of the gas and the geometric description of the compressor, the mass flow and the gas temperature in the compressor has to be known. This data is provided by Compressor1d and Compressor2d. In addition, if the wall temperatures are specified the total heat fluxes can be calculated.

The comparisons between Compressor1d and full three dimensional solutions can be found in figure 15.

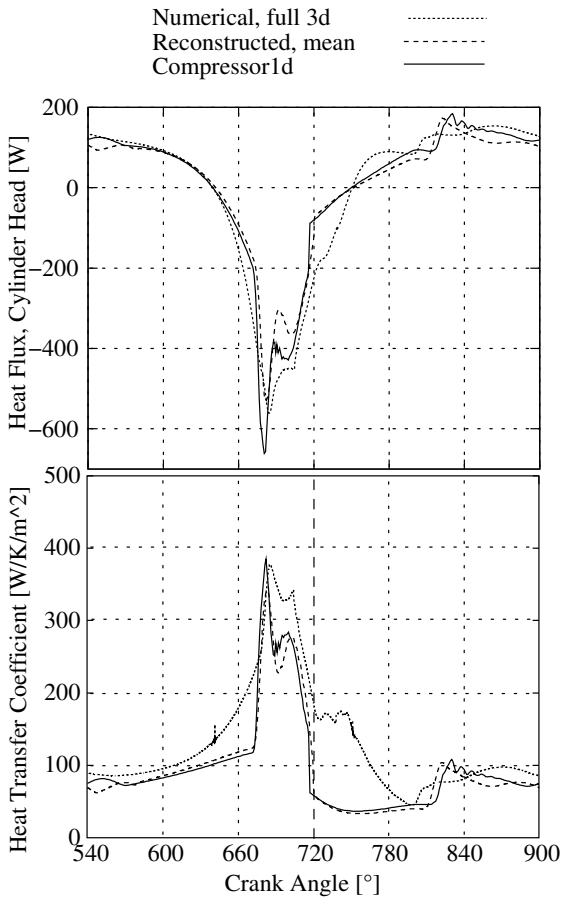

Figure 15: Heat flux and corresponding heat flux coefficient for the cylinder head

5 Conclusion

In the project 'Modelling Fluid Dynamics, Heat Transfer and Valve Dynamics in a Reciprocating Compressor' sponsored by the EFRC a one-dimensional and a two-dimensional gas flow model and a simplified heat transfer calculation are introduced. It turns out that these models are sufficient to capture the main characteristics of the compressor.

Future research will include expanding the range of validity of the heat transfer model to different compressor types. In addition we will conduct measurements of heat fluxes on a test compressor.

6 Acknowledgements

The research is financed by the European Forum for Reciprocating Compressors. The authors want to thank F. Newman (Ariel), G. Machu and P. Steinrück (Hoerbiger) and G. Samland and D. Sauter (Burckhardt Compression) for many fruitful discussions.

References

[1] Meyer, G. (2004): Simulation der Strömung in einem Kolbenverdichter. Diplomarbeit, TU-Wien.

[2] Aigner, R. Meyer, G., Steinrück H. (2005): Valve Dynamics and Internal Waves in a Reciprocating Compressor. 4th EFRC-Conference, 169-178.

[3] Costagliola, M. (1950): The Theory for Spring Loaded Valves for Reciprocating Compressors. J. Appl. Mech, 415-420.

[4] Zierep, J. (1997): Grundzüge der Strömungslehre. Springer Berlin Heidelberg.

[5] Leveque, R. (2004): Finite Volume Methods for Hyperbolic Problems. Cambridge University Press.

[6] Lax, P. D., Wendroff, B. (1960): System of Conservation Laws. Comp. Pure and Appl. Math., 13, 217-237.